Eur Biophys J (1999) 28: 312–316

ARTICLE

M. Lekka · P. Laidler · D. Gil · J. Lekki · Z. Stachura
A.Z. Hrynkiewicz

Elasticity of normal and cancerous human bladder cells studied by scanning force microscopy

Received: 30 April 1998 / Revised version: 17 December 1998 / Accepted: 21 January 1999

Abstract Scanning force microscopy was used for the determination of the elastic properties of living cells in their culture conditions. The studies were carried out on human epithelial cells. Two similar lines of normal cells (Hu609 and HCV29) and three cancerous ones (Hu456, T24, BC3726) were measured using the scanning force microscope in order to collect the force versus indentation curves. The BC3726 line originates from the HCV29 cell line which was transformed by the *v-ras* oncogene. To evaluate their elastic properties, Young's modulus values were determined. The present study has shown that normal cells have a Young's modulus of about one order of magnitude higher than cancerous ones. Such a change might be attributed to a difference in the organisation of cell cytoskeletons and requires further studies.

Key words Scanning force microscopy · Cytoskeleton elasticity · Normal and cancerous cells

Introduction

The mechanical properties of cells (adhesion, viscoelasticity) have been investigated using many different methods based on the qualitative observation of the cells, behaviour controlled by different factors causing their deformation. Only a few methods provide quantitative information about cell mechanical properties [for example, the micromanipulation technique (Leriève et al. 1995) or optical tweezers (Svoboda et al. 1992)]. Recently, the scanning force microscope (SFM, Binnig et al. 1986; Lal and Scott 1994) has become a very useful tool in biological studies. It can provide three-dimensional images of cell surfaces with resolution comparable to that obtained in electron microscopy. A significant advantage of the SFM is that measurements can be performed on living objects in their natural aqueous environment. In addition to imaging, SFM brings also a possibility of direct measurements of the interaction between a probing tip and the cell surface, simply by indenting it. Quantitative analysis of the elastic properties is possible by analysing force-distance curves (Radmacher 1997). In this way, information about the elastic properties of the investigated cell can be obtained, and the resulting conclusions may be extended to the cytoskeletal structure inside the cell (Hoh and Schoenenberger 1994; Ricci et al. 1997).

The internal structure of most cells is governed by the cytoskeleton. One of its basic components is an actin cortex that consists of actin filaments directly underlying the cell membrane attached via numerous membrane proteins. The cortex can extend up to about 0.5–1 μm below the cell membrane (Skalak 1992). The cytoskeleton plays an important role in cell division, locomotion and transport of intracellular particles (Janmey 1995). Oncogenically transformed cells differ from normal ones in many ways. Differences in cell growth, morphology, cell-to-cell interaction and also in cell membrane and organisation of the cytoskeleton have been reported (Ben-Ze'ev 1985; Rao and Cohen 1991). These differences should cause changes in the mechanical properties of the cell. In order to confirm this thesis, the elasticity of cells coming from the normal and transformed bladder epithelium was studied.

Materials and methods

SFM sample preparation started from special treatment of the glass coverslip substrate (Menzel-Gläser, 24 mm×24 mm). This was done in the following way: a clean glass coverslip was immersed into 1 μg/ml poly-L-lysine solution (PLL, Sigma) for 5 min. This increased the number of amino groups, causing better adhesion of cells to the glass substrate (Hartmann and Galla 1978). Next, the glass

M. Lekka (✉) · J. Lekki · Z. Stachura · A.Z. Hrynkiewicz
Institute of Nuclear Physics, Radzikowskiego 152,
PL-31-342 Cracow, Poland
e-mail: lekka@alf.ifj.edu.pl

P. Laidler · D. Gil
Institute of Medical Biochemistry Collegium Medicum, UJ,
Kopernika 7, PL-31-034 Cracow, Poland

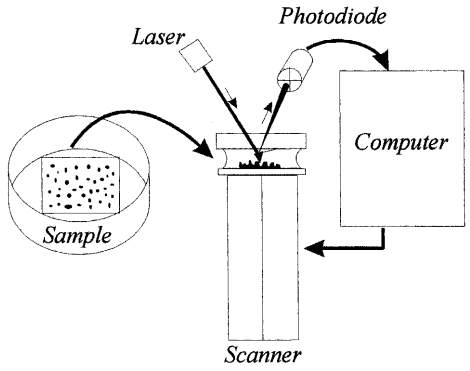

Fig. 1 Schematic view of scanning force microscopy setup using the liquid cell and laser deflection technique

coverslip was dried in a clean atmosphere for 24 h at room temperature.

The following cell lines were chosen for the SFM measurements: Hu609 (non-malignant ureter) and Hu456 (bladder transitional cell carcinoma) (cells obtained from Institute of Immunology and Experimental Therapy, PAN, Wrocław, Poland), HCV29 (non-malignant bladder urothelium) and BC3726 (HCV29 cells transfected with *v-ras* oncogene) (cell lines established in Fibiger Institute, Copenhagen, Denmark) and T24 (bladder transitional cell carcinoma) (ATCC HTB4).

All types of cells of the bladder epithelium were grown at 37°C in a 95% air/5% CO_2 incubator (ASSAB). They were grown in RPMI1640 medium (pH 7.4, Sigma) containing 10% fetal calf serum (FCS, Böhringer). The cells were taken after the same number of passages, and then they were cultured on glass coverslips prepared as described above. Only Hu456 cells were grown on glass coverslips without any adhesive factor. No fixation or drying step was involved during sample preparation. After the growing cells formed the monolayer they were taken for measurements.

A home-built scanning force microscope was used in the experiment (Lekka et al. 1996). It was equipped with a scanner (Staveley Sensor) with a maximum *XY* scan range of 20 μm×20 μm, and a *Z* range of ±1.5 μm. Commercial Si_3N_4 cantilevers were used (Park Scientific Instruments). Spring constants of 0.1, 0.03 and 0.05 N/m were chosen. Tip radii were about 20–30 nm, which were checked using a standard TGT01 silicon grating (NMDT, Molecular Devices and Tools for Nanotechnology, Moscow). A home-made plexiglass "liquid cell" without the "O-ring" sealing was used. Cell measurements were performed in RPMI medium containing 10% FCS at room temperature. The coverslip with cells (still immersed in the RPMI medium) was put into the "liquid cell" placed on an SFM scanner (see the schematic view of the force microscope in Fig. 1). The cell was localised using an optical microscope, and the tip was moved towards the cell centre in order to avoid the influence of the substrate and the neighbouring cells. Cell migration during the measurement was negligible and was checked by cell imaging. Every culture was measured several times using a new tip and fresh medium. In order to perform the measurements in conditions close to physiological ones, an average experiment lasted no more than 2 h. At room temperature and in ambient air, cells preserved their viability for more than 3 h and were checked by Trypan Blue staining.

Data analysis

Force curves reflecting the interaction between the probing tip and the cell surface were collected using the laser deflection technique. In this case, the piezo scanner only elongates in the direction towards the surface and backwards (*Z* direction). The *XY* scanning function of the scanner was disabled. The force scale was obtained by multiplying the cantilever deflection by the spring constant. A separate calibration was performed for each series of curves taken in the same session both before and after the measurement. In the range of the applied force (up to 20 nN) there is no significant glass deformation caused by the SFM tip, and therefore the glass sample was used as the calibration reference, assuming its infinitesimal stiffness. Cell indentation was obtained by comparing the experimental curve with the corresponding curve for the reference glass sample. In these experiments, force curves were collected with a step of 1.2 nm at an average speed of 190 nm/s. In order to evaluate the deformability of the cells, Young's modulus was determined using Sneddon's mechanics (Sneddon 1965). This model describes the elastic behaviour of the elastic half-space being pushed by a hard axisymmetric indenter. The cell surface can be modelled by an elastic half-space since the range of the indentation was up to 1.6 μm in comparison with the thickness cell of 10–14 μm. The SFM tip can be approximated by a cone (Radmacher et al. 1995) or paraboloid with the radius of curvature *R* at the apex (Weisenhorn et al. 1993). Both models are not limited by a finite tip end radius (unlike the classical Hertz model describing the interaction of a sphere with flat surface) and may be extended for large indentation depths. For this analysis the model assuming a paraboloidal tip shape was chosen. Following this model, sample indentation Δz depends on the acting force F, the geometry of the tip and material properties according to the equation:

$$F = \frac{4}{3}\sqrt{R}\,E'\,\Delta z^{1.5} \tag{1}$$

where E' is a reduced Young's modulus of the tip-cell sample system:

$$\frac{1}{E'} = \frac{1-\mu_{\text{tip}}^2}{E_{\text{tip}}} + \frac{1-\mu_{\text{cell}}^2}{E_{\text{cell}}} \tag{2}$$

and E_{tip}, E_{cell} are Young's moduli of the tip and the cell, while μ_{tip}, μ_{cell} are Poisson ratios. Taking into account that $E_{\text{tip}} \gg E_{\text{cell}}$, one obtains finally:

$$E' = \frac{E_{\text{cell}}}{1-\mu_{\text{cell}}^2} \tag{3}$$

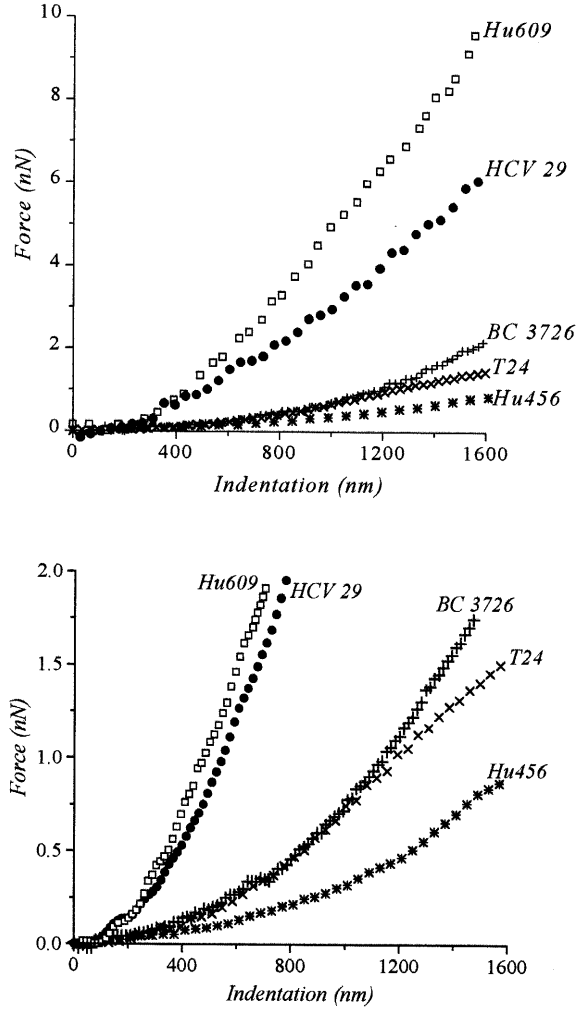

Fig. 2 Comparison of force versus indentation curves taken for normal (Hu609 and HCV29) and for cancerous cell lines (Hu456, BC3726, T24) for **a** a high load (up to 10 nN) and **b** a low load (up to 2 nN)

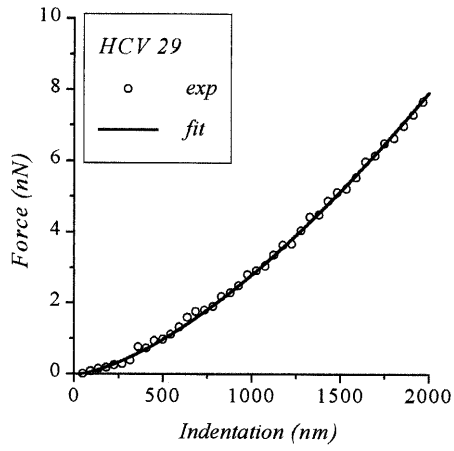

Fig. 3 Indentation versus force curve for HCV29 cells. *Open circles* experimental data, *solid line* fit following the physical model assuming a paraboloidal tip indenting the elastic half-space

Table 1 Young's moduli calculated for measured cell lines. The last column gives the information about the number of force curves taken into account[a]

Cell line	Young's modulus (kPa) $\mu_{cell}=0$	Young's modulus (kPa) $\mu_{cell}=0.5$	Number of analysed force curves
Hu609	12.9 (±4.8)	9.7 (±3.6)	325
HCV29	10.0 (±4.6)	7.5 (±3.6)	121
BC3726	1.4 (±0.7)	1.0 (±0.6)	214
T24	1.0 (±0.5)	0.8 (±0.4)	201
Hu456	0.4 (±0.3)	0.3 (±0.2)	10

[a] The total number of measured cells is about 20 cells for each line

Results

During contact between the tip and the investigated sample, the tip pushes on the sample. On a hard surface, tip movement towards the sample produces the same amount of cantilever deflection. It is different in the case of force curves measured for cells that show deformation of their surface upon a loading force when the tip approaches the surface. Comparison between reference calibration and cell measurements allows one to determine the cell indentation and to construct force versus indentation plots. Force versus indentation curves of normal and cancerous cells are shown in Fig. 2. High load (up to 10 nN) curves are shown in Fig. 2a, while Fig. 2b shows data points corresponding to low loads up to 2 nN.

Results for two normal, epithelial cell lines coming from a non-malignant ureter (Hu609) and from a non-malignant bladder urothelium (HCV29) differ significantly from these obtained for cancerous cell lines (BC3726, T24, Hu456). The force required for indentation of normal cells is much higher than that for cancerous cells. This phenomenon indicates that normal cells are significantly stiffer than the latter ones.

To evaluate differences in the force versus indentation behaviour, Young's moduli were determined by fitting Eq. (1) to the experimental data. An example of the experimental indentation curve and the fitted function is shown in Fig. 3.

Calculated Young's modulus values are presented in Table 1. Table values were obtained by fitting a Gauss distribution to histograms (Fig. 4) for 100–300 separate measurements performed for about 20 cells for each line. Errors correspond to the half width of the gaussian peak. A typical gaussian peak corresponding to single cell results was narrower (about 30%) than for the total histograms presented in Fig. 4. During the experiment (up to 2 h of measurement session) no systematic change in acquired data was observed.

Curves taken on several different cultures of the same cell line show reasonable reproducibility. The standard *t*-test (0.05 level) confirmed significant differences between Young's moduli for normal and cancerous cell populations and insignificant differences within analogous cell populations. Results for Hu456 cells were obtained in a pi-

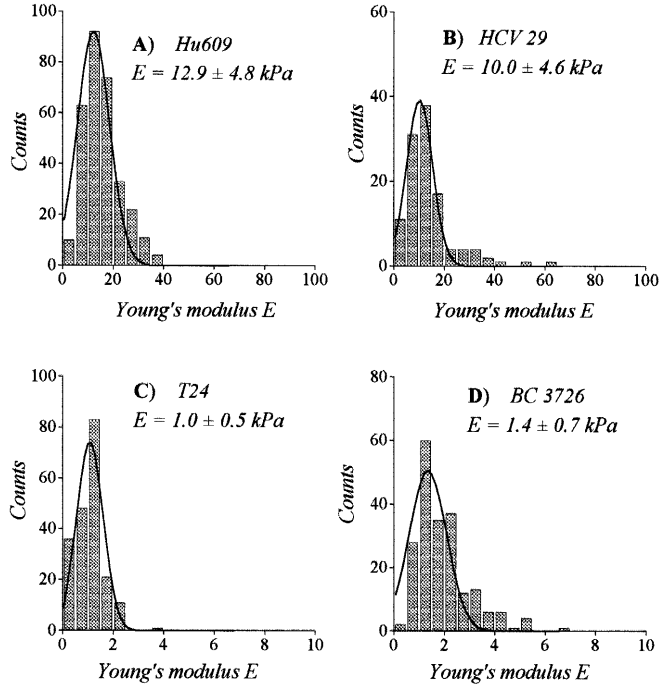

Fig. 4 Histograms showing the mean value and the distribution of Young's moduli measured for normal (**A, B**) and cancerous (**C, D**) cells. In this evaluation it was assumed that the Poisson ratio is $\mu_{cell}=0$ (see discussion of measurement errors)

lot experiment, and therefore contain a low number of measurements (in the pilot measurement, Hu456 cells were compared with normal cells Hu609).

Discussion

The measurements of the elastic properties of normal and cancerous cell lines were carried out with special care to ensure similar experimental conditions (identical chemical, the same adhesive factor, etc.). Only the cell line Hu456 was grown without any adhesive factor. However, despite this difference and the low statistics, its calculated Young's modulus value fits well with the overall results.

Calculated Young's moduli form two distinct groups: values about 10 kPa are characteristic for normal cells and values about 1kPa for cancerous cells. This allows us to quantify differences between the cells. A comparison of the Young's moduli of the normal and cancerous cells shows that the latter are significantly less stiff and easier to deform. The applied forces (up to 10 nN) and indentation depths (up to 1.6 μm) are large compared to some other studies (Radmacher et al. 1995). However, in several publications the loading forces in the range of 5–10 nN have been successfully applied in the investigation of living cells (Hofmann et al. 1997; Braet et al. 1998). The destruction of the cell surface caused by the high load was improbable because of the very good reproducibility of the multiple force curves sequentially measured at the same place. The other possible source of error was the influence of the hard glass coverslip substrate. This factor was neglected owing to the large cell thickness, ranging from 10 μm to 14 μm. Additionally, the analysis performed for lower forces (up to 2 nN) produces close Young's modulus values. For example, the Young's modulus for the normal lines Hu609 calculated for lower load forces (up 2 nN) is 15.2±4.7 kPa versus 12.9±4.8 kPa obtained for large forces. The Young's moduli calculated for cancerous cell lines also remain almost the same when calculated for small indentation depths and low loads.

Cells are very soft objects, and therefore cell indentation depends on the response from the glycocalix, from the cell membrane and from the cytoskeleton. For small indentation values (lower than 100 nm), when the influence of the membrane is the highest, the difference between normal and cancerous cells is not visible. We may therefore assume that using this method at present we can not draw conclusions concerning normal and cancerous cell membrane structures. The difference between normal and cancerous cells becomes apparent with the increase of the intendation. Comparison of the dimensions of all the interacting objects and the indentation depth suggests that the response of the cellular scaffold is most important, and therefore the elastic properties measured reflect mainly the properties of the cytoskeleton. Quantitatively determined differences in the elastic properties between normal and cancerous cells were attributed to possible changes in cytoskeleton organisation due to oncogenic transformation.

This observation supports the results obtained for measured fibroblasts by various manipulation techniques (Thoumine and Ott 1997), where the normal fibroblasts showed lower deformability than their SV40 transformed counterparts. Also, Goldman et al. reported that the vinculin-deficient F9 mouse embryonic carcinoma cells had a lower Young's modulus than the wild-type cells, when measured by atomic force microscopy. The authors attributed these changes to an altered cytoskeletal organisation (Goldmann et al. 1995; Goldmann and Ezzel 1996). A low stiffness of cancer cells may be caused by a partial loss of actin filaments and/or microtubules, and therefore by a lower density of the cellular scaffold. Poor differentiation of the cell, including the cytoskeleton and reduced adhesive interactions, characterise the vast majority of cancer cells (Ben-Ze'ev 1997). The measurement of Young's modulus of the cells can in future help to determine the range of cytoskeleton changes and allow us to quantify them.

In addition to the approximations of the applied physical model of the interaction between the pushing tip and the investigated surface, measurement errors originate from the following factors:

- To ensure similar experimental conditions, measurements were performed at several points close to the cell centre. This was done because the forces versus indentation curves depend on which part of a cell they were collected from: the middle or close to the cell's edge (Ricci and Grattarola 1994). However, discrepancies arising from

inhomogeneities of the cell membrane and of the cell age could not be avoided.

- All calculations were performed assuming a fixed tip radius R of 25 nm and nominal values of spring force constants k. In practice, these properties of scanning tips differ even for tips carefully chosen from the same series of production. Thanks to the relatively high statistics, even a large possible spread of the tip radii and spring constants does not alter the conclusions of the present study. For example, a significant change of the tip radius R from 25 to 35 nm introduces a decrease in Young's modulus of only 15%.
- The Poisson ratio is a characteristic material property, of a value ranging between 0 and 0.5. Its real value for cells is difficult to estimate. Therefore, two columns in Table 1 show limiting values of Young's moduli calculated for this range. Nevertheless, we do not expect significant differences in the Poisson's ratio for similar types of cells.

However, the observed changes were so significant that for the high statistics of the results, all the above possible errors and uncertainties have little influence on the final conclusions.

Acknowledgements We would like to thank Prof. J. Stachura from the Department of Pathomorphology, Collegium Medicum, UJ, for helpful remarks and discussions. This work was partially supported by the State Committee for Scientific Research (KBN), Grant No. 2 P03B03312, and by the State Committee for Scientific Research (Collegium Medicum, UJ), No. 501/Pk/3/L.

References

Ben-Ze'ev A (1985) The cytoskeleton in cancer cells. Biochim Biophys Acta 780: 197–212

Ben-Ze'ev A (1997) Cytoskeletal and adhesion proteins as tumor suppressors. Curr Opin Cell Biol 9: 99–108

Binnig G, Quate CF, Gerber C (1986) Atomic force microscope. Phys Rev Lett 56: 930–933

Braet F, Rotsch C, Wise E, Radmacher M (1998) Comparison of fixed and living endothelial cells by atomic force microscopy. Appl Phys A 66: S575–S578

Goldmann WH, Schindl M, Cardozo TJ, Ezzell RM (1995) Motility of viculin-deficient F9 embryonic carcinoma cells analyzed by video, laser confocal, and reflection interference contrast microscopy. Exp Cell Res 221: 311–319

Goldmann WH, Ezzel RM (1996) Viscoelasticity in wild-type and viculin-deficient (5.51) mouse F9 embryonic carcinoma cells examined by atomic force microscopy and rheology. Exp Cell Res 226: 234–237

Hartmann W, Galla HJ (1978) Binding of polylysine to charged bilayer membranes: molecular organization of a lipid-peptide complex. Biochim Biophys Acta 509: 474–490

Hofmann UG, Rotsch Ch, Parak WJ, Radmacher M (1997) Investigating the cytoskeleton of chicken cardiocytes with the atomic force microscope. J Struct Biol 119: 84–91

Hoh J, Schoenenberger CA (1994) Surface morphology and mechanical properties of MDCK monolayers by atomic force microscopy. J Cell Sci 107: 1105–1114

Janmey P (1995) Cell membranes and the cytoskeleton. In: Lipowsky R, Sackmann E (eds) Structure and dynamics of membranes. Elsevier, Amsterdam

Lal R, John SA (1994) Biological applications of atomic force microscopy. Invited review no. 0193-1894/94, American Physiological Society. Am J Physiol 266: C1–21

Lekka M, Lekki J, Shoulyarenko AP, Cleff B, Stachura J, Stachura Z (1996) Scanning force microscopy of biological samples. Pol J Pathol 47: 51–55

Lerièvе J, Bucherer C, Geiger S, Lacombe C, Vereycken V (1995) Blood cell mechanics evaluated by the single-cell micromanipulation. J Phys III 5: 1689–1706

Radmacher M (1997) Measuring the elastic properties of biological samples with the AFM. IEEE Eng Med Biol 16 (2): 47–57

Radmacher M, Fritz M, Hansma PK (1995) Imaging soft samples with the atomic force microscope: gelatin in water and propanol. Biophys J 69: 264–270

Rao K, Cohen H (1991) Actin cytoskeletal network in aging and cancer. Mutat Res 256: 139–148

Ricci D, Grattarola M (1994) Scanning force microscopy on lived cultured cells: imaging and force-versus-distance investigations. J Microsc 176: 254–261

Ricci D, Tedesco M, Grattarola M (1997) Mechanical and morphological properties of living 3T6 cells probed via scanning force microscopy. Microsc Res Techn 36: 165–171

Skalak R (1992) Cellular biomechanics. In: Trigg GL (ed) Encyclopedia of applied physics, vol 3. VCH, Weinheim

Sneddon IN (1965) The relation between load and penetration in axisymmetric Boussinesq problem for a punch of arbitrary profile. Int J Eng Sci 3: 47–57

Svoboda K, Schmidt CF, Branton B, Block SM (1992) Conformation and elasticity of the isolated red blood cell membrane skeleton. Biophys J 63: 784–793

Thoumine O, Ott A (1997) Comparison of the mechanical properties of normal and transformed fibroblasts. Biorheology 34: 309–326

Weisenhorn A, Khorsandi M, Kasas S, Gotzos V, Butt HJ (1993) Deformation and height anomaly of soft surfaces studied with an AFM. Nanotechnology 4: 106–113